Chemical Engineering Journal 165 (2010) 336–346

Contents lists available at ScienceDirect

Chemical Engineering Journal

journal homepage: www.elsevier.com/locate/cej

Support effect over bimetallic ruthenium–promoter catalysts in hydrogenation reactions

J. Fontana[a], C. Vignado[a], E. Jordão[a], W.A. Carvalho[b,*]

[a] *Laboratory of Catalytic Processes Development, Chemical Systems Engineering Department, Faculty of Chemical Engineering, Universidade Estadual de Campinas, Cidade Universitária Zeferino Vaz, CP. 6066, CEP 13083-970, Campinas, SP, Brazil*

[b] *Centro de Ciências Naturais e Humanas, Universidade Federal do ABC, Rua Santa Adélia, 166, CEP 09210-170, Santo André, SP, Brazil*

ARTICLE INFO

Article history:
Received 7 May 2010
Received in revised form 28 August 2010
Accepted 10 September 2010

Keywords:
Hydrogenation
Ruthenium
Diol
Bimetallic catalyst
SMSI

ABSTRACT

The present work evaluates the influence of RuSn catalyst supported on La_2O_3, TiO_2, SiO_2 and Nb_2O_5 in dimethyl adipate (DMA) hydrogenation to obtain 1,6-hexanodiol. The catalysts were prepared by impregnation method, calcined and reduced at 673 K. The reactions were carried out in liquid phase in a Parr high pressure reactor at 528 K and 50 bar. The catalysts supported on SiO_2 and Nb_2O_5 show higher selectivity to diol, 59% and 50% and conversion of 57% and 28%, respectively, indicating that the new active phases formed in the metal–support interface are able to hydrogenate the DMA ester group. The presence of positively charged tin species acting as Lewis acid sites could be considered as responsible for the carbonyl activation. It is also verified that a synergic effect between promoter and support is extremely important for the formation of 1,6-hexanediol.

1. Introduction

Diols are di-substituted alcohols obtained from the hydrogenation of esters and dicarboxylic acids. The reactivity of these carbonyl compounds follows the following order of reactivity: aldehydes > esters > carboxylic acids, according to the susceptibility to nucleophilic attack. The hydrogenation of carbonyl compounds, especially esters, is difficult due to the polar nature of the C=O bond which is weakly polarizable and make esters less reactives.

Moreover, the presence of the alkyl group adjacent to the ester carbonyl group can cause steric hindrance. It makes the reaction complex and causes changes in the activity and selectivity of the catalysts, also justifying the high pressures and temperatures used in these hydrogenation processes. Therefore, the production of diols under milder reaction requires more active catalysts.

The 1,6-hexanodiol (diol) is a valuable intermediary for the chemical industry. It has applications in the synthesis of some polymers and it is also used in fine chemistry. This linear diol contains two hydroxyl terminal groups. Such configuration results in a fast and simultaneous reaction for the formation of disubstituted products. The 1,6-hexanodiol is used in the polyesters production for elastomers of polyurethane, coverings, adhesives and plasticizers [1].

The catalysts used in hydrogenation of C=O group are made from metals of group VIII (Os, Ir, Pt, Ru, Rh). According to Ponec [2] these metals can be presented in the following order of selectivity and hydrogenation of C=O bond in aldehydes α,β-unsaturated: Os ~ Ir > Pt > Ru > Rh. However, when monometallic or not promoted catalysts are used, the selectivity is generally low. Both activity and selectivity can be influenced by the support used and the addition of a second metal.

In previous studies [3–6] we evaluated the activity and selectivity of monometallic catalysts of Pd, Rh, Pt and Ru supported on alumina, titania, and pillared clays. For the catalysts supported on alumina, ruthenium showed higher activity in the hydrogenation of dimethyl adipate, reaching about 80% conversion. However, there was no production of 1,6-hexanodiol. The catalysts of Pt, Pd and Rh produced larger quantities of undesirable products such as alcohols and hydrocarbons over the ruthenium catalyst which showed a smaller range of products and high selectivity to the formation of the monomethyl ester of adipic acid, MME (70%). It was concluded that, in this system, the metallic sites are responsible for breaking the selective $O–CH_3$ bond of the ester group [3].

The presence of tin was essential to promote and change the chemical selectivity of bimetallic catalysts. In monometallic catalyst sites of ruthenium led to the formation of MME by breaking the $O–CH_3$ bond. Adding tin, the catalyst produced 1,6-hexanediol. This better performance was attributed to the presence of Lewis acid sites, Sn^{n+} on the surface of the catalyst. The presence of tin in the ruthenium catalyst led to a relatively small decrease in catalytic activity. This effect was explained by the blocking of the

---

[*] Corresponding author. Tel.: +55 11 4996 0174; fax: +55 11 4996 0174.
E-mail address: wagner.carvalho@ufabc.edu.br (W.A. Carvalho).

1385-8947/$ – see front matter © 2010 Elsevier B.V. All rights reserved.
doi:10.1016/j.cej.2010.09.050

sites of ruthenium surface by tin, which does not adsorb molecular hydrogen atoms of adjacent ruthenium [4,5]. By using Sn/Al_2O_3 as catalyst low activity for the hydrogenation reaction under study was obtained, reaching 16% after 10 h reaction time [5]. There was also the formation of ε-caprolactone (CPL), suggesting that its production does not depend on metallic sites and may be obtained from the intramolecular esterification of DMA, related to the presence of acid species in the reaction medium. Lewis acid sites present on the alumina surface could be the active sites of the catalyst. The bimetallic catalyst supported on alumina has proven to be suitable for the production of 1,6-hexanediol from DMA, and the presence of tin species are not the ones responsible by the catalyst activity. The preparation method is also extremely important and it determines the location of species that would generate SnO_x, which are the precursors of the selective $RuSnO_x$ sites [5].

In supported metal catalysts, the support not only modifies the metal dispersion, but there are also metal–support interactions due to physical and chemical properties of both. Examples are the electron transfer for the formation of chemical bonds, interaction forces like Van der Waals, deposition of reduced species of support on the metal surface or the formation of new phases on the surface. The interaction between the substrate and dispersed metal can strongly influence the adsorptive and catalytic properties of the catalyst and is not based solely on the nature of the compounds involved, but also in the method used to support the metal as a heat treatment step [1]. Thus, the choice of the support emphasizes the importance of evaluating some intrinsic features of the various materials such as, for example, the surface area, porosity and mechanical resistance and chemical operating conditions. There are several inorganic materials that meet these requirements and can be used in the preparation of catalysts. However, despite the full range of solids available, in practice only three have been used industrially, alumina, silica and coal [7].

In recent years, the concept of strong metal support interaction, SMSI, has gained considerable importance, since the nature of support can cause changes in the catalyst performance. Initially observed with TiO_2 [8], the SMSI effect may be present in several other reducible oxides such as MnO, V_2O_5, Nb_2O_5, La_2O_3 and CeO_2 [9]. The application of niobium pentoxide (Nb_2O_5) or niobia as support is interesting since its abundance on Earth is about 20 ppm, while Brazil is a major producer with 60% of world production, followed by Canada, Nigeria and Zaire [10]. The applications of niobia in various catalytic processes can be found both as support of metal catalysts and as promoters, interacting with other metals [10]. Niobia is a reducible oxide subject to SMSI, and the migration of support reduced species to the surface of active metal particles can alter the activity and selectivity of the catalyst.

In this work, it was reported the support effect in the hydrogenation of DMA on bimetallic ruthenium–promoter based catalyst systems to obtain 1,6-hexanediol. The supports tested were La_2O_3, TiO_2 and Nb_2O_5, known as reducible oxides, and SiO_2, an unreducible oxide. The catalysts were obtained by impregnation method and characterized by BET, XRD, TPR and EDS. The combined effect of tin and support species on 1,6-hexanediol production and the influence of different chemical nature of the support on the formation of the active sites were investigated.

2. Experimental

2.1. Preparation of catalysts

Catalysts were prepared by the impregnation method in aqueous suspensions, in order to obtain a solid with nominal concentration of 2 wt% in ruthenium and 4.7 wt% in tin. Supports applied here were TiO_2 (rutile phase, Synth), $La(OH)_3$ (Aldrich), Nb_2O_5 (Aldrich) and SiO_2 (Alfa) crushed and sieved to the average fraction of 0.045 mm. Precursor salts used were $RuCl_3{\cdot}0.5H_2O$ (Aldrich, 98%) and $SnCl_2{\cdot}2H_2O$ (Aldrich 98%). The impregnation was done by adding the support and the solution containing the metallic precursors in a flask placed onto the rotative evaporator with bath at 333 K and vacuum for 5 h. Next, solid was oven dried for 12 h, at a temperature of 393 K. Catalysts were then subjected to calcination treatment for 4 h at 673 K, under 50 mL min^{-1} of synthetic air flow, and reduction for 2 h at 673 K, under flow of 40 mL min^{-1} of 2% H_2 and 98% N_2 mixture.

2.2. Characterization

A Micromeritics ASAP 2010 device was used to obtain adsorption–desorption measurements at 77 K, under pressure ranging from 10 to 925 mmHg. Before each measurement the samples were outgassed at 423 K and 1.3×10^{-3} Pa for 12 h. Specific areas were obtained according to Brunauer, Emmett and Teller (BET) method.

Diffractograms were obtained in a Phillips model X'Pert diffractometer, equipped with graphite monochromator and a rotative sampler. Spectra were registered between $2\theta = 10^\circ$ and 100°, with scanning speed of $0.02^\circ\ \theta\ min^{-1}$, using a cathode current of 50 mA and a voltage of 40 kV. The radiation used was Cu Kα radiation ($\lambda = 1.5418$ Å), The angular velocity of the goniometer was $0.02^\circ\ 2\theta$ and time of 0.4 s, and the usual interval scanning was $2\theta = 2$–35°.

Analysis of temperature programmed reduction (TPR) was performed in a Quantachrome Chembet300 device. Samples were held on a quartz reactor, using 50 mg of each catalyst under flow of reductive gas mixture containing 5% hydrogen and 95% nitrogen, at outflow of 80 mL min^{-1}. Analysis of temperature was programmed to vary from 298 to 1273 K, with heating rate of 10 K min^{-1}.

A scanning electron microscope LEICA, Stereoscan 440 was used. An Oxford 7060 detector, coupled to the microscope, provided the elemental local composition by energy-dispersive electron probe X-ray analysis.

2.3. Catalytic tests

Dimethyl adipate hydrogenation was held on a high pressure 300 mL stirred batch Parr reactor (Model 4566), made of AISI 316 stainless tin equipped with mechanical agitation axis and speed controller. Reactions were carried out in liquid medium with 1,4-dioxane as suitable solvent to keep the reaction phase homogeneity. The system was kept at 523 K and 50 atm of H_2, under constant 1500 rpm mechanical stirring. Typically, 1.40 g of catalyst, 80 mL of 1,4-dioxane, 7.09 g of dimethyl adipate and 1.8 g of tetradecane (internal standard) were used. Samples were collected for each reaction along 15 h.

Reaction products quantification was done by using gas chromatography through a HP6890 chromatograph equipped with a capillary column 100% polyethylene glycol and for internal standard, tetradecane. Identification of the main products was previously held in a gas chromatograph attached to a Shimadzu CGMS QP2010 Plus mass spectrometer (GC–MS).

3. Results and discussion

3.1. Characterization of catalysts

Fig. 1 shows the X-ray diffraction of the support, La_2O_3, and the catalyst $RuSn/La_2O_3$. The crystalline phase present in the support consists of lanthanum oxide (La_2O_3) and lanthanum trihydroxide ($La(OH)_3$), as indicated in the diffractogram. Trihydroxide formation occurs through contact between the original oxide and moisture. According to Rosynek and Magnuson [11], the transition

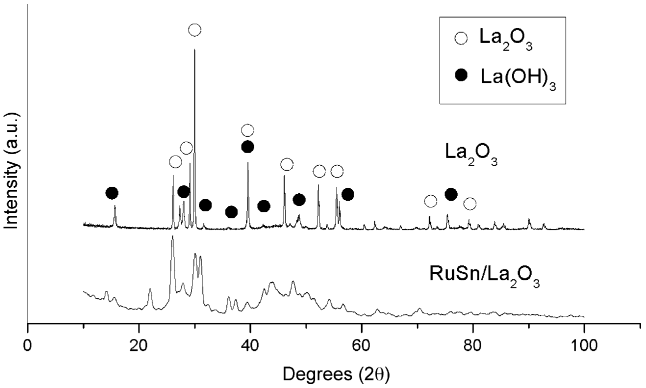

Fig. 1. X-ray diffractogram of the support La_2O_3 and $RuSn/La_2O_3$ catalyst.

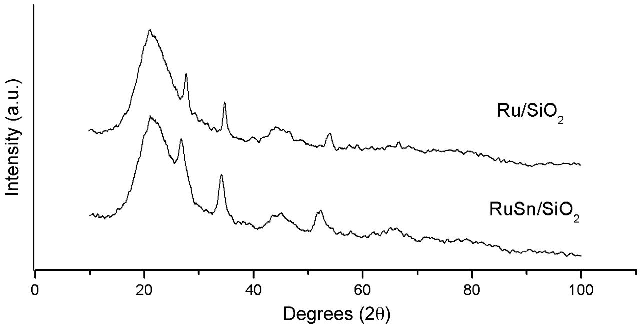

Fig. 3. X-ray diffractogram of the support SiO_2 and $RuSn/SiO_2$ catalyst.

from oxide to hydroxide is preferred to the formation of surface hydroxyl groups, usually found in oxides such as alumina and silica. This assumption was confirmed by thermogravimetric analysis (not presented in this work) that shows the presence of trihydroxide.

By comparing the diffractograms of La_2O_3 and $RuSn/La_2O_3$, there are changes in the structure of the solid. After the impregnation of metal precursors, the solid presented low crystallinity along the investigated angular range, and it was not possible to identify crystalline phases for both ruthenium and tin. The metal impregnation process was carried out in aqueous solution under heating. This may have favored the partial conversion of the crystalline oxide structure to the corresponding amorphous hydroxide. Thermogravimetric analysis (not shown in this work) indicated a mass loss around 596 K, corresponding to the decomposition of $La(OH)_3$ and possible formation of an intermediate LaO(OH). Around 763 K this oxyhydroxide specie suffers dehydration, leading to the formation of La_2O_3. These results are similar to those found by Taylor and Schrader [12], which indicate the transition of $La(OH)_3$ to LaO(OH) around 623 K. In this temperature is also possible the presence of La_2O_3. However, the full transition of these species to oxide occurs around 823 K, while the calcination process of the sample was done at 673 K. Thus, the crystallinity of the solid was reduced after the metals impregnation, even after submit the material to the calcination process.

Fig. 2 shows the X-ray diffraction of TiO_2 and $RuSn/TiO_2$. The impregnation of metals in the support did not alter the crystallinity of the material and was not possible to identify metallic crystalline phases. Possibly, the absence of crystallographic peaks related to both ruthenium and tin may be due to their low concentration in these catalysts, especially ruthenium (<2 wt%) or to the presence of the oxides in an amorphous and highly dispersed phase on the support surface [1]. The support corresponds to the TiO_2 rutile phase (TiO_2–R). Rutile phase is characterized by being more thermally stable compared to the anatase phase, most commonly used in catalysis. Thus, rutile presents lower metal–support interaction and would be less susceptible to the SMSI effect, since the reduction of ionic species Ti(IV) to Ti(III), would be difficult in this phase [13]. Consistent with this assumption are the results of hydrogenation of DMA presented by Silva et al. [14] when studying RuSn catalysts supported on TiO_2 (anatase).

Fig. 3 shows the XRD patterns of silica, characteristic of amorphous structures, and its respective catalyst $RuSn/SiO_2$. In this case it is possible to observe peaks attributed to ruthenium oxide RuO_2 at 2θ 26.76° and 34.07°, unlike other catalysts studied, where the metallic phase cannot be detected. This behavior may be associated with different sizes of RuO_2 particles caused by the different nature of the support and the different crystallinities of the RuO_2 phase in each catalyst. As verified by TPR analysis, shown below, the interaction between ruthenium and silica is smaller than its interaction with lantania, for example. Given this little interaction, it would be expected larger particle size of ruthenium when it is supported on SiO_2 due to greater mobility of metal species, which could lead to increased particle aggregation.

The diffractograms of niobia and $RuSn/Nb_2O_5$ are shown in Fig. 4, where we can see that the angular position and the interplanar distances of peaks lines are identical for both diffractograms. There are, however, small decreases in the intensity of the peaks.

Table 1 shows the values of specific surface area and pore volumes of the supports and catalysts. The range of solids surface area is between 0.6 and 15.5 $m^2\,g^{-1}$. These values are much smaller than those typically found in supports such as alumina and activated charcoal. Thus, the differences found in the catalytic behavior and other effects that may be related to the support would be mainly due to the nature of the support and not to differences in surface

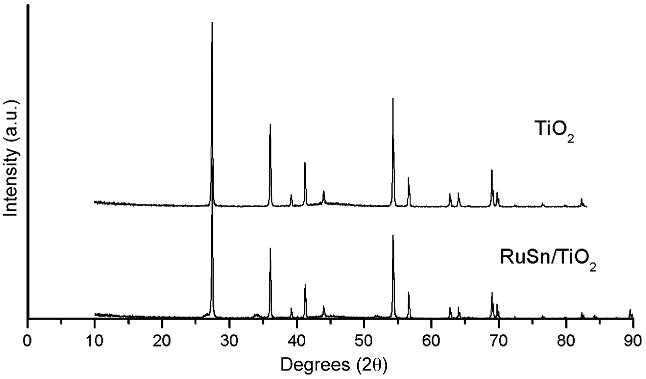

Fig. 2. X-ray diffractogram of the support TiO_2 and $RuSn/TiO_2$ catalyst.

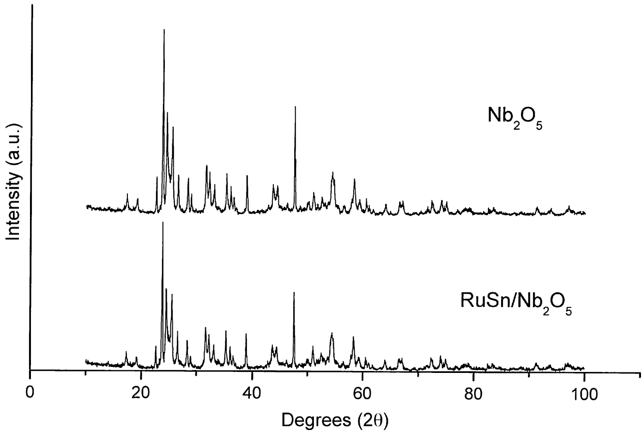

Fig. 4. X-ray diffractogram of the support Nb_2O_5 and $RuSn/Nb_2O_5$ catalyst.

Table 1
Specific surface area (SA) and pore volume (PV) of the media.

Solid	SA ($m^2 g^{-1}$)	PV ($cm^3 g^{-1}$)
La_2O_3	7.1	0.02
TiO_2–R	15.5	0.3
SiO_2	8.3	0.02
Nb_2O_5	0.6	nd
RuSn/La_2O_3	9.5	0.03
RuSn/TiO_2–R	12.8	0.3
RuSn/SiO_2	8.4	0.02
RuSn/Nb_2O_5	0.6	nd

nd: not determined.

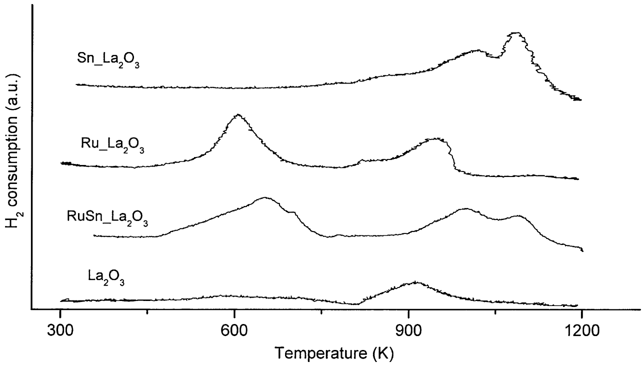

Fig. 5. TPR profile for La_2O_3, RuSn/La_2O_3, Ru/La_2O_3 and Sn/La_2O_3.

areas. Bimetallic catalysts supported on niobia, silica and titania present no significant variation of specific surface areas after the impregnation method of metal precursors in low-level concentration and the calcination process. Moreover, such behavior is to be expected considering the nearly absence of porous structures in the solids used as support [4,15].

The specific surface area found in the lantania (7.1 $m^2 g^{-1}$) is consistent with the area obtained by Rosynek and Magnuson [11] for the pure La_2O_3 (7.5 $m^2 g^{-1}$), while $La(OH)_3$ has specific surface area of 18.5 $m^2 g^{-1}$. It is suggested that the phase La_2O_3 is predominant in the solid used as support. After impregnation and calcination processes, lantania supported catalyst presented a specific surface area 34% higher than the support (9.5 $m^2 g^{-1}$). This indicates that some structural change occurs, but it maintains La_2O_3 as the predominant phase. Regarding to the low surface area found in the niobia sample, in fact, the values for the oxide found in the literature vary a lot, from 1.9 $m^2 g^{-1}$ [16] to 132 $m^2 g^{-1}$ in a review by Ziolek [17].

The reduction profiles of bimetallic catalysts show significant differences in behavior of metal–promoter interactions. Temperatures of hydrogen consumption peaks are functions of the metal and the strength of their adsorption sites. The shift of these peaks in the temperature range may indicate a metal–support interaction, metal–metal or the formation of a new phase as an alloy in the case of bimetallic catalysts. The adopted parameter is that the higher the temperature of reduction of components in supported catalysts, the greater the interaction between the metal and support [18].

Fig. 5 shows the reduction profiles of lantania and the systems Ru/La_2O_3, Sn/La_2O_3 and RuSn/La_2O_3 calcined.TPR of RuSn/La_2O_3 is very close to the overlap of the profiles of monometallic catalysts Ru/La_2O_3 and Sn/La_2O_3. This behavior indicates that there was little interaction between the metals, probably caused by the strong interaction between each metal with the support, as verified in the monometallic catalysts. The catalytic tests presented below show that the catalyst RuSn/La_2O_3 had low activity and selectivity compared to other catalysts. This could be explained by the incomplete reduction of the tin, which would have remained in the oxide form in the employed reducing conditions. This oxide species is not able of activating the carbonyl. However, an increase in the peak, corresponding to the reduction observed in the ruthenium bimetallic catalyst, may indicate the possibility of reduction of low amounts of tin due to the presence of ruthenium. This fact would justify the formation of diol by this catalyst.

The peaks of hydrogen consumption in between 873 K and 1023 K in the reduction profiles of catalysts supported on La_2O_3 were attributed to the reduction of the support. Some authors also associate this peak to the decomposition of carbonate species like $La_2(CO_3)_3$ and $La_2O_2CO_3$, that occur in the same temperature range, around 923 K [19,20]. The ease interaction of lanthanide oxides with atmospheric CO_2 justify the presence of these species, which have already been identified through mass spectrometry by Bernal et al. [21]. However, there was no evidence of these species in the X-ray diffraction in this work or in other works taken as a reference, although they do not exclude the possibility of the presence of carbonate phase.

Tin modifies somewhat the reducibility of the support, since the reduction of the support in the Sn/La_2O_3 sample begins around 873 K, with maximum around 1023 K; while in the absence of tin reduction occurs around 913 K. In the presence of ruthenium (Ru/La_2O_3) there was an increase in the reduction temperature of the support, but to a lesser extent. La_2O_3 reduction takes place around 953 K, representing a displacement of 313 K for the pure support, while in the bimetallic sample RuSn/La_2O_3, the reduction of La_2O_3 was around 983 K (a shift of 70 K). The increase in temperature reduction of the La_2O_3 may be associated with the interaction of the support with metals, mainly through electronic interactions with tin ions.

In addition to changes as a result of phase transitions from $La(OH)_3$ to La_2O_3, it must be consider that part of the lantania may still be reduced simultaneously with ruthenium and tin, since there is an easier partial reduction of reducible oxides present near the metal by hydrogen spillover. In this case, the species of partially reduced support can be deposited on the surface of the active metal, leading to a fall in the rate of hydrogen chemisorption and then a decrease in activity, characterizing the so-called decorative effect, shown in Fig. 6.

Fig. 7 shows the reduction profiles of the systems supported on TiO_2–R: Ru/TiO_2–R, Sn/TiO_2–R and RuSn/TiO_2–R. The TPR of the support TiO_2–R is not shown once it did not show peaks of hydrogen consumption in the analysis conditions.

Comparatively, the reduction profiles of the systems supported on TiO_2–R allow to deduce that there is a combined influence of promoter and support in the formation of the active phase. Differ-

Fig. 6. Decorative effect: the migration of reduced species (LaO_x) on the active metal surface.

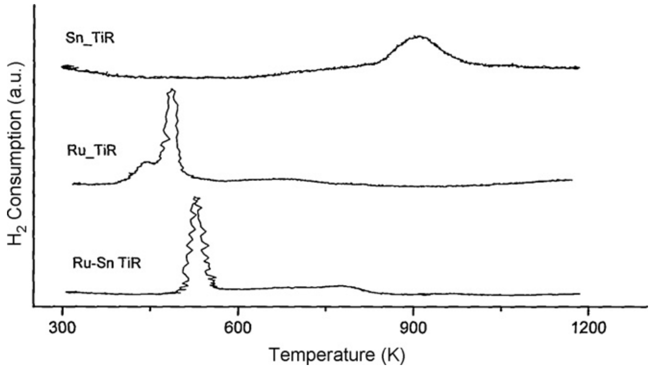

Fig. 7. TPR profile for RuSn/TiO_2–R, Ru/TiO_2–R and Sn/TiO_2–R.

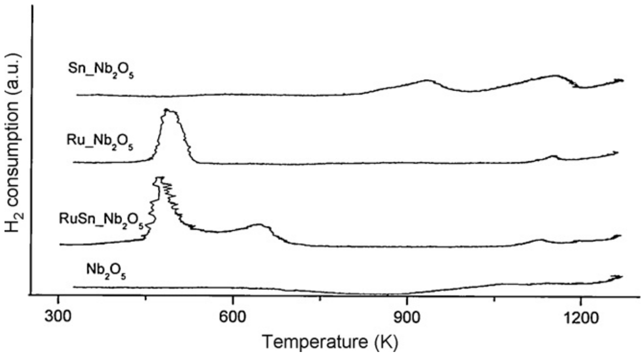

Fig. 9. TPR profile for Nb_2O_5, RuSn/Nb_2O_5, Ru/Nb_2O_5 and Sn/Nb_2O_5.

ent sites present in solid surface may change the interaction with the active metal, as well as in the oxidation state of the promoter (tin), reflecting the catalytic properties. This may lead to the formation of specific sites in the metal–support interface. Unlike the behavior shown when using La_2O_3, the metal–promoter interaction stood out the metal–support interaction, of both ruthenium and tin, contributing to a decrease in the reduction temperature.

The reduction profile of the catalyst RuSn/TiO_2–R is completely different from the overlap of monometallic catalysts profiles, showing an increase in the consumption of hydrogen, slightly shifted to higher temperature (528 K) than that observed in the sample Ru/TiO_2–R. It is not possible to distinguish different reduction stages of metals, suggesting that they occur simultaneously. This observation highlights the effective interaction between ruthenium and tin provided by the nature of the support, with the possibility of keeping all the tin in direct contact with the ruthenium atoms. Thus, tin could be catalytically reduced by hydrogen spillover from ruthenium. There is also the hypothesis of the formation of a new phase characterized by an alloy Ru_xSn_y, which also shows a reduction profile containing only one peak of hydrogen consumption [22,23]. Based on the results of the catalytic tests presented below, this new phase formed either by the presence of ionic tin alone or as an alloy, proved to be very active, rather than selective to the formation of diol. According to Pouilloux et al. [23], when used as an alloy with noble metal, tin would be positively charged by the electrons transfer from the less noble metal to the nobler one, and the difference in the electronegativity between the metals may also promote the polarization of the C=O bond.

The reduction profiles of monometallic and bimetallic systems supported on SiO_2 are shown in Fig. 8. Similar to the behavior of TiO_2–R, the TPR of SiO_2 did not show peaks of hydrogen consumption in the analyzed conditions.

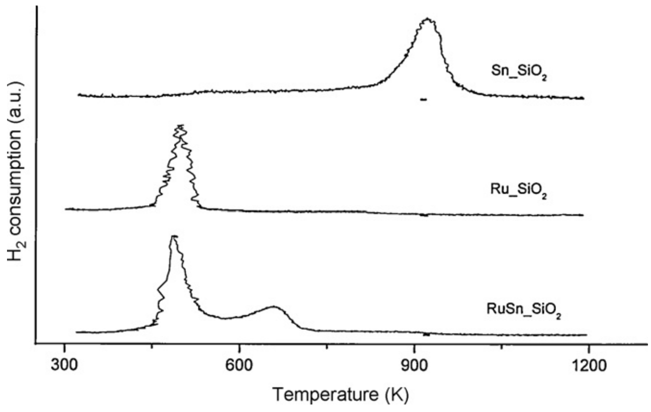

Fig. 8. TPR profile for RuSn/SiO_2, Ru/SiO_2 and Sn/SiO_2.

It may be observed that the profile of the bimetallic RuSn/SiO_2 sample is completely different from the profiles of the monometallic samples, indicating a high degree of metal–promoter interaction regarding to metal–support interaction. This smaller interaction of the support with both ruthenium and tin provided a greater interaction between the metals, leading to lower reduction temperatures, especially for tin.

Tin is reduced at a very low temperature with the bimetallic catalyst (RuSn/SiO_2), around 658 K; while in the absence of ruthenium (Sn/SiO_2), the reduction occurs at 918 K. This shift of about 533 K is the result of a possible direct or indirect interaction between the metals. The reduction of tin must be favored by ruthenium or through spillover of hydrogen from ruthenium. Some authors, among them Pouilloux et al. [23] and Riguetto et al. [24], verified the presence of metallic tin in a RuSn/SiO_2 catalyst after reduction at high temperature (around 773 K). According to Riguetto et al. [24], these cationic species would be formed through reoxidation processes. The presence of two peaks of hydrogen consumption in the reduction profile of RuSn/SiO_2 contradicts the possibility of forming a RuSn alloy. The results indicate the reduction of two different metal species, with the first peak related to reduction of ruthenium and the second, to tin. However, in this case the oxidation state of tin species present after the reduction is uncertain.

The presence of tin did not significantly modify the temperature of reduction of the ruthenium in the RuSn/SiO_2 sample (483 K) regarding the monometallic Ru/SiO_2 (498 K). Llorca et al. [25] attributed the small shift to a lower temperature of reduction to an increase of ruthenium dispersion in the presence of tin oxides. Thus, it can be suggested that the tin may slightly have changed the dispersion of active metal in the system supported on SiO_2. Kluson and Cervany [26] explain the increase in the dispersion after addition of tin by the existence of SnO and SnO_2 species interacting with Ru(0), where they act as spacers between the sites of the metal in its metallic state.

Fig. 9 shows the reduction profiles of niobia and their supported catalysts: Ru/Nb_2O_5, Sn/Nb_2O_5 and RuSn/Nb_2O_5.

It is observed that niobia is reduced in a wide temperature range, starting above 923 K. Catalysts reduction profiles showed that in the presence of metals, particularly ruthenium, the support's partial reduction is shifted to a higher temperature starting the reduction at around 1073 K. In fact, Wachs et al. [16] describes that the reduction of niobia starts at around 1073 K reaching up to 1573 K. Noronha et al. [18] showed a partial reduction of niobia around 1200 K in the presence of palladium in catalysts Pd/Nb_2O_5. According to the authors, the reduction of niobia blocks the active surface of the metal, decreasing the chemisorption of H_2 and the activity of the catalyst.

Besides the evident reduction of niobia at elevated temperatures, its reduction can also occur simultaneously with the reduction of metals, due to the SMSI effect. The NbO_x species

Table 2
Concentration of the main components of bimetallic catalysts, obtained by EDS.

Catalyst	Concentration (%)			
	Ruthenium	Tin	Chlorine	Ru/Sn ratio
$RuSn/La_2O_3$	1.6	3.3	1.8	2.0
$RuSn/TiO_2$–R	1.6	3.2	0.1	2.0
$RuSn/SiO_2$	1.1	2.0	Nd[a]	1.8
$RuSn/Nb_2O_5$	1.4	2.5	Nd[a]	1.8

[a] Not detected.

could cause the effect of decoration, blocking metallic active sites and inhibiting the excessive substrate's hydrogenation. This may be related to the scarce formation of byproducts in the catalytic tests and to the lower activity presented by the bimetallic catalyst regarding the use of the support as catalyst.

The TPR of the $RuSn/Nb_2O_5$ sample is very similar to $RuSn/SiO_2$. As in SiO_2 supported catalyst, $RuSn/Nb_2O_5$ reduction profile is quite different from the superposition of the monometallic catalysts profiles, especially concerning the tin reduction. This metal has its reduction peak shifted from about 563 K to a temperature lower than that for the monometallic catalyst Sn/Nb_2O_5. This remark shows that the interaction between tin and niobia is less effective, allowing greater interaction between the metals. Tin reduction is favored in the vicinity of ruthenium for a possible spillover of hydrogen. Moreover, the presence of two peaks of reduction precludes the possibility of RuSn alloys formation.

Reduction temperature of ruthenium in bimetallic catalyst (473 K) decreased slightly, about 10 K regarding the monometallic catalyst. Once again, we have an indication of a possible increase, even small, of the dispersion by the presence of tin oxide species. As the $RuSn/SiO_2$ catalyst, the oxidation state of tin is uncertain. However, it is suggested that ionic tin species are present during the reaction.

As we have seeing in the catalytic tests, it is clear that the sites obtained by the use of $RuSn/SiO_2$ and $RuSn/Nb_2O_5$ catalysts are suitable for the hydrogenation of the ester group of DMA, leading to the formation of 1,6-hexanediol. The high selectivity to 1,6-hexanediol was attributed to tin species acting as Lewis acids near the active metal particles, provided by tin reduction. Lewis acid sites favor the adsorption of the substrate through the interaction with the pair of free electrons of oxygen, thus increasing the possibility of hydrogenation of the C=O bond. In fact, this is the most appropriate explanation consistent with several previous studies of the promoting effect on the selectivity of reactions involving the presence of positively charged ionic groups [2,27–30].

Microscopy analysis were performed using EDS (energy dispersive electron probe X-ray analysis) with elemental mapping, which provided an approximate value of the concentration of metals dispersed on the support, as well as chlorine remaining after the calcination process.

Table 2 shows the averages obtained from three readings of mapping from different areas of the sample by EDS.

It is observed that there is no chlorine in the catalysts supported on TiO_2–R, SiO_2 and Nb_2O_5 after the calcination process, while the catalyst supported on La_2O_3 remains with 1.8% of chlorine. The levels of ruthenium and tin present in all samples were below the nominal levels of these metals, while the metals ratios showed values close to the expected ones.

3.2. Catalytic tests

Fig. 10 provides DMA concentration curves for systems without catalyst (blank) and with supported catalysts. The concentration is related to overall catalytic activity of the catalyst after 15 h reaction time.

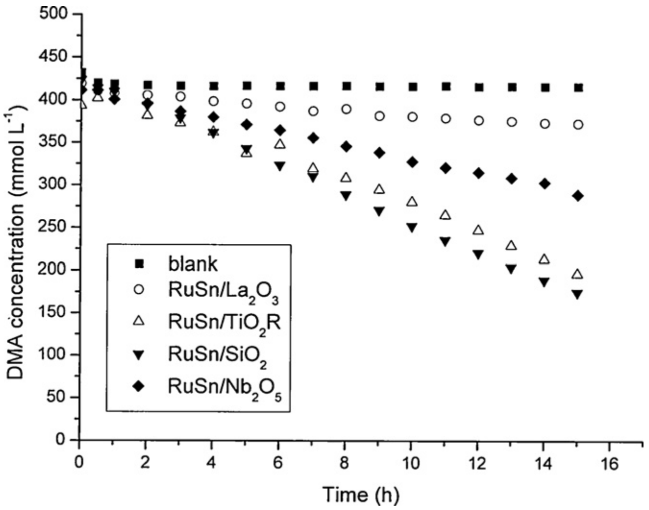

Fig. 10. Dimethyl adipate concentration in function of time.

In the blank, the maximum DMA conversion occurs in the first hour, remaining constant after that. In the bimetallic catalytic systems the concentration of DMA decreases steadily and did not reach the equilibrium after 15 h reaction time.

Clearly the presented conversions indicate that the catalytic activity is affected by the support. Many factors can be responsible for these behaviors. One would be the difference in surface area presented by the oxides, which can alter the distribution of active metal on the support [31]. However, since the oxides used as supports in this study did not show high surface areas, as verified by BET analysis, it was assumed that the influence of this parameter is smaller. Another factor was the chemical nature of the solid, which can significantly influence the performance of the catalyst due to the formation of new active sites by metal–support interaction, as indicated by TPR analysis.

Given that the reducible oxides including TiO_2–R, La_2O_3 and Nb_2O_5 are subject to the SMSI phenomenon, characterized by the formation of partially reduced oxide species (LaO_x, TiO_x and NbO_x), the lowest conversion of DMA were obtained by catalysts supported on La_2O_3 and Nb_2O_5. Although titania is also a reducible oxide, XRD results have shown that the titanium oxide corresponds to the rutile phase. According to the literature, rutile is less likely susceptible to the SMSI effect than anatase and therefore the formation of species responsible for the decoration effect and the decrease in catalytic activity is favored [32]. The same applies to the use of silica as support, because it is not a reducible oxide.

On the other hand, it is known that the use of reducible supports can lead to an increase in the rate of hydrogenation by facilitating the activation of C=O bond [33]. Previous results also show that the presence of TiO_x species located on the metal–support interface is essential for the selectivity to diol. These species inhibit excessive hydrogenation of substrate molecules, since they would be responsible to disable active sites related to side reactions. In fact, it was observed in studies performed by Silva et al. [5], where the catalyst supported on Al_2O_3, which is not susceptible to the SMSI effect, provides a very high conversion (90%), but the selectivity to diol reached only 6%. This value can be considered low when compared to the reducible oxides, suggesting that the presence of partially reduced species of the support could improve the selectivity of the reaction.

Table 3 shows the selectivity values obtained after 15 h reaction time. Products not identified in this work are named as "other" and their concentrations were determined by the difference between the consumption of DMA and the sum of the identified products.

Table 3
Selectivity to products formed by catalytic hydrogenation of DMA after 15 h reaction time.

Catalyst	Conv. (%)	Selectivity (%)						
		1-ol	Hex. ac.	CPL	Diol	MHH	MME	Other
$RuSn/La_2O_3$	8.9	1.5	–	10.4	9.7	–	2.4	75.9
Ru/La_2O_3	52.4	–	–	–	1.1	–	27.9	68.9
Sn/La_2O_3	17.1	–	–	–	2.2	–	1.8	95.9
$RuSn/TiO_2$–R	51.5	0.8	0.9	3.3	19.1	12.2	0.6	63.2
Ru/TiO_2–R	16.7	–	2.8	8.1	5.6	0.1	26.9	47.5
Sn/TiO_2–R	11.5	–	–	–	3.3	–	25.2	71.6
$RuSn/SiO_2$	56.6	0.3	–	2.0	59.3	9.7	6.6	21.2
Ru/SiO_2	6.2	–	5.9	5.2	5.8	8.3	25.2	66.4
Sn/SiO_2	13.2	–	–	–	–	2.8	2.2	24.8
$RuSn/Nb_2O_5$	28.5	–	–	4.4	50.5	18.1	25.0	1.9
Ru/Nb_2O_5	15.5	–	–	–	14.0	23.6	12.6	45.9
Sn/Nb_2O_5	5.9	–	–	–	10.1	2.9	57.9	28.9

1-ol: 1-hexanol; Hex. Ac.: hexanoic acid; CPL: ε-caprolactone; Diol: 1,6-hexanediol; MHH: methyl 6-hydroxy-hexanoate; MME: adipic acid monomethyl ester.

This difference could already be related to products absorbed into the structure of the catalyst or gas phase, preventing their detection in the employed analytical conditions. The distribution of products is related to a change in surface sites of metal catalysts, in accordance with the oxide used as support, especially regarding the formation of the product of interest 1,6-hexanediol.

Catalytic tests were performed using only the support as catalysts. A particular property of these systems was the formation of MME. The system catalyzed by La_2O_3 showed 9.8% substrate conversion and 3% of selectivity to the MME, corresponding to 1.5 mmol L^{-1}. Systems TiO_2–R, SiO_2 and Nb_2O_5 presented conversions of 7.4%, 14.2% and 2.9% with selectivity to the MME of 57.5% (17.3 mmol L^{-1}), 100% (57.3 mmol L^{-1}) and 71% (19.5 mmol L^{-1}), respectively. Although previous studies attribute the breaking of the O–CH_3 bond to sites of metallic ruthenium, it is believed that they are not solely responsible for the formation of MME in the supported catalysts. The results indicate that the support may also be capable of promoting hydrogenolysis of O–CH_3 bond. It is suggested that this ability is related to acid strength displayed by the solids, which present the following order of acidity: $SiO_2 > Nb_2O_5 > TiO_2 > La_2O_3$. It appears that the higher the support acid strength, the higher the selectivity to MME in these catalysts. This proposal is more evident when the results are compared with literature data related to tin monometallic catalysts and acid studies conducted by Auroux et al. [34] and Figueiredo et al. [35]. According to the authors, the MgO, considered as basic as La_2O_3, had an increase of acid sites in the presence of SnO_2. Accordingly, in this work we observed an increase in conversion and formation of MME by the Sn/La_2O_3 catalyst. The insertion of tin in TiO_2–R did not significantly alter its acid strength, since there was no significant change in the formation of MME as well as in the DMA conversion. However, it is shown that tin somewhat modifies the behavior of the catalysts leading to the consumption of MME during the reaction, differently of what happens in tests using only the support as catalysts.

According to studies by Auroux et al. [34] alumina, known for its acid properties, may have its acid strength increased or decreased according to the tin content in the catalyst. Thus, it is suggested that the tin content used in this study (~4%) may have reduced the acid character of silica, lowering the formation of the monoester in the catalyst Sn/SiO_2.

The value of substrate conversion in the bimetallic system $RuSn/La_2O_3$ is much smaller than that showed by the catalyst Ru/La_2O_3. This result indicates changes in the catalytic sites in the presence of tin from the bimetallic catalyst. Such behavior may be associated to TPR results of $RuSn/La_2O_3$ (Fig. 5). It was observed that the reduction condition used in the catalyst preparation (673 K) is not enough to reduce much of the tin oxide present in the sample. Thus, the low activity presented may indicate decoration or encapsulation of the ruthenium particles by tin oxides. As in the case of decoration promoted by support reduced species (Fig. 6), the blocking of active metallic sites responsible for the dissociation of hydrogen can occur. The migration of tin oxides particles to the ruthenium surface can result in the decline of the hydrogenation rate [28]. This behavior was also verified by Pouilloux et al. [29] with RuSn catalysts, inferring also the decrease in activity.

The results indicate that the catalyst Ru/La_2O_3 is more active and selective to MME than pure La_2O_3. It is assumed that this behavior is related to an increase in the amount of hydrogen dissociated by the presence of metallic ruthenium in the monometallic ruthenium catalyst. However, when using Ru/La_2O_3, there was an induction period of 8 h. The catalyst Sn/La_2O_3 showed 10% of selectivity to MME after 6 h reaction time. Thereafter, the selectivity decreases, indicating that MME is being partially converted to 1,6-hexanediol and especially "other".

The distribution of the products obtained by $RuSn/La_2O_3$ catalyst (Fig. 11), indicates as main products CPL and diol. The increase in concentration of both products occurs throughout 15 h reaction time.

The formation of diol can occur by hydrogenation of CPL, MME or MHH. However, it is suggested that by using the catalyst

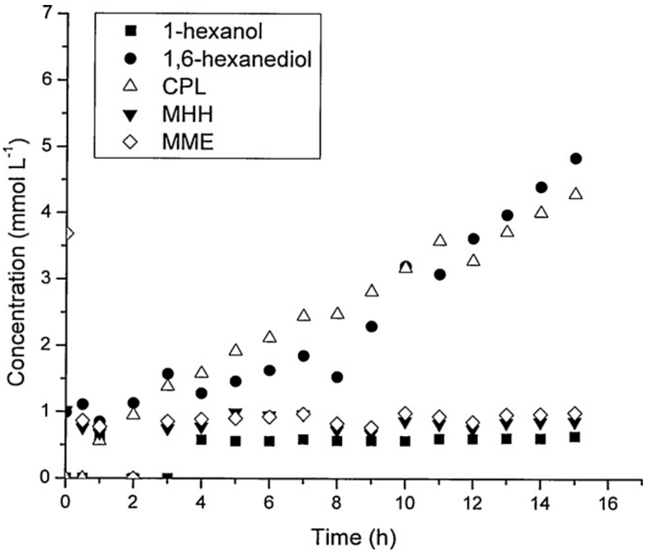

Fig. 11. Products obtained with catalyst $RuSn/La_2O_3$ [(■) 1-hexanol, (△) caprolactone, (●) methyl 6-hydroxyhexanoate, (○)adipic acid monomethyl ester, (▲) 1,6-hexanediol].

$RuSn/La_2O_3$, the formation of diol occurs by direct hydrogenation of the substrate [Eq. (1)], since it was not observed the consumption of intermediate products.

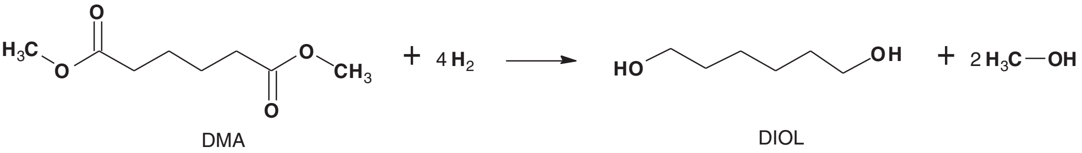

(1)

The formation of cyclic products such as CPL can be influenced by the acid nature of some solids [5]. CPL can be formed by either DMA hydrogenation or intramolecular transesterification, due to the presence of H^+ species in the reaction media, illustrated by Eqs. (2) and (3), respectively. However, considering the basic character of this support (La_2O_3), the formation of CPL can be attributed solely to the hydrogenation of DMA followed by intramolecular nucleophilic addition of the intermediate MHH. Moreover, it is possible to identify a correlation between acidity and the formation of lactone in the results obtained with other catalysts.

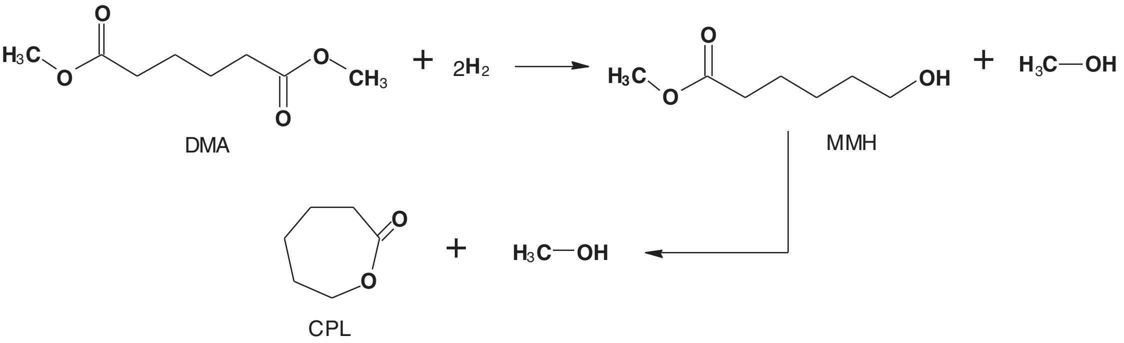

(2)

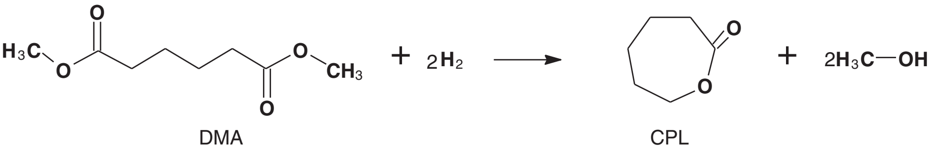

(3)

Ru/TiO_2–R and Sn/TiO_2–R showed relatively low conversions compared with $RuSn/TiO_2$–R catalyst. It is suggested that in the absence of tin (Ru/TiO_2–R), hydrogen dissociated by active metal does not react efficiently with the carbonyl of DMA due to the low reactivity of the ester group. This process would be effective due to a promoting effect caused by species of the support (such as TiO_x, where $1.5 < x < 2$) in close contact with the active metal in the ruthenium metal–support interface. These species could also be responsible by the polarization of the carbonyl [31]. Accordingly, Poondi and Vannice [36] suggest that partially reduced TiO_2–R species have contributed to the selectivity in the hydrogenation of carbonyl when platinum catalysts were subjected to high reduction temperature. Although the rutile phase is considered more thermally stable, results of catalytic tests for the catalysts supported on TiO_2–R suggest the presence of TiO_x species in the reaction medium. On the other hand, the role of cationic species of the support is not considered very effective in the polarization of the carbonyl. The major contribution is attributed to the presence of metallic cations as promoters of Lewis acid sites, which can be observed when comparing the results obtained with Ru/TiO_2–R and $RuSn/TiO_2$–R regarding the diol selectivity. As already mentioned, cationic tin species act as electron acceptors. These species favor the adsorption of substrate molecules on the surface of the catalyst, since this interaction occurs through oxygen atoms from carbonyl. Therefore, the bond strength between metals and oxygen reflects on the catalytic properties. According to Tahara et al. [27], the increase in the rate of hydrogenation of C═O bond due to the presence of tin species on the surface of the catalyst is caused by the strong interaction between oxygen atoms of the carbonyl group and tin sites. This interaction can be evidenced by the heat formation of SnO_2 ($-239.3\ kJ\ mol^{-1}$), which is higher than that of RuO_2 ($-285.8\ kJ\ mol^{-1}$), so the affinity of tin to oxygen will be greater than that of ruthenium.

Fig. 12 shows the kinetic behavior of the bimetallic $RuSn/TiO_2$–R catalyst, where the main products are diol and MHH.

The formation of MHH concomitant with diol, both with high selectivity, indicates the ability of the catalyst to promote two reactions [Eq. (4)]. They must be present distinct catalytically active species, since the carboxyl group remaining after the first

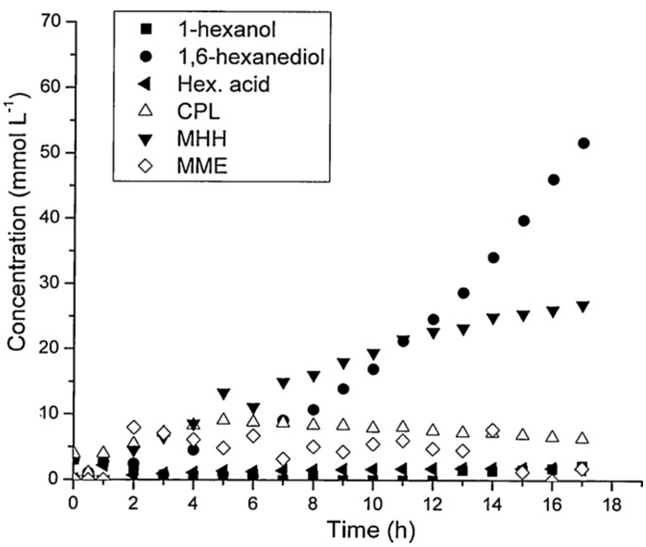

Fig. 12. Products obtained with catalyst $RuSn/TiO_2$–R.

hydrogenolysis is more stabilized and thus less susceptible to hydrogenation.

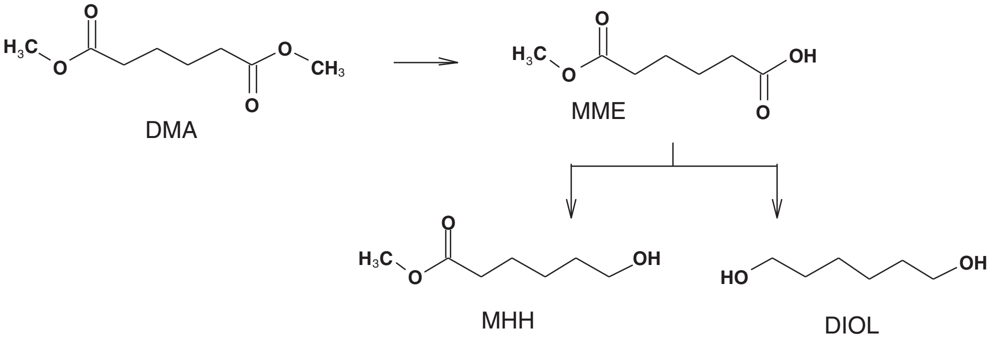

(4)

CPL production occurs in the first 5 h reaction time and remains constant. Since the support TiO_2–R presents a weak acid character [37], the formation of CPL should be given only by the DMA hydrogenation. MME is produced in the first 2 h reaction time. Thereafter, its concentration begins to decrease, with possible conversion to both diol and MHH. MME can be an intermediate product of DMA reaction, where it is formed and rapidly converted into other reaction products [1]. The production of 1-ol occurs within the first hours of reaction and remains almost constant throughout 15 h. The formation of hexanoic acid begins in the third hour of reaction, and may have been formed by hydrogenation of intermediate products or by direct DMA hydrogenation [Eq. (5)].

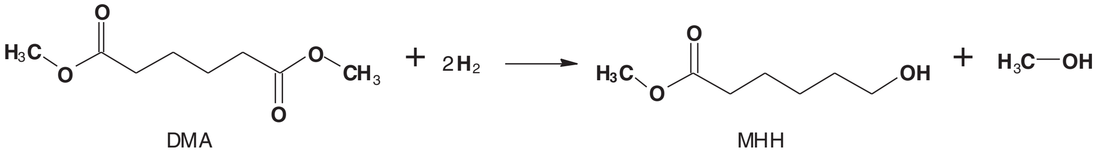

(6)

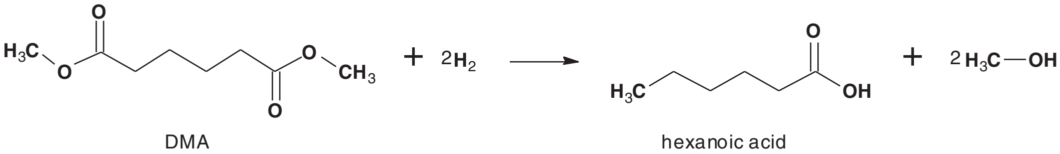

(5)

As observed in the TiO_2–R supported systems, a considerable increase in catalytic activity occurs when bimetallic catalyst supported on SiO_2 is tested. The activity is 10 times greater than that observed with the monometallic catalyst, which can be attributed to the presence of tin. In the case of monometallic catalyst Ru/SiO_2, it is noteworthy that silica is not a reducible oxide and therefore it is not expected the formation of partially reduced species of the support acting as Lewis acid sites. Therefore, as already suggested for the system Ru/TiO_2–R, the presented low conversion suggests a deficiency in the ability to activate C=O bond.

The results of silica catalysts are contrasting with the results presented by alumina support as shown by Silva et al. [5]. Although silica and alumina are both not reducible, silica-supported catalyst showed significant selectivity to diol. This result may be related to the reducibility of tin species on silica, observed by TPR, which could be contributing to the selectivity of the catalyst through the formation of selective sites. In the case of alumina, it may be formed complex [Sn^{2+}-alumina] and tin oxides stabilized on the surface, that cannot be reduced easily [14]. This suggests that the metal–support interaction must be able of creating active catalytic sites, but should not inhibit both the adsorption of hydrogen in metal particles and the metal–promoter interaction.

Fig. 13 shows the formation of products catalyzed by RuSn/SiO_2 which showed to be very promising in the DMA hydrogenation, making it attractive to obtain diol. Therefore, it should be noted that the reaction was conducted at 50 atm, relatively low compared to the pressures commonly used in industrial processes to obtain such products. Compared to studies on monometallic catalysts, it is observed that the presence of tin in the catalyst is critical in order to obtain adequate selectivity to diol, with low formation of byproducts, mainly MME.

Production of MHH increases over the 15 h reaction time and may occur according to Eq. (6).

The decrease in MME selectivity by RuSn/SiO_2 catalyst may indicate that part of the formed product acts as an intermediate of the reaction, being instantly consumed for production of other substances such as diol. This behavior was associated with an increased reactivity of the C=O group due to the presence of tin ionic species. However, it was not elucidated the oxidation state of tin species, although the total reduction of tin to the metallic state can occur.

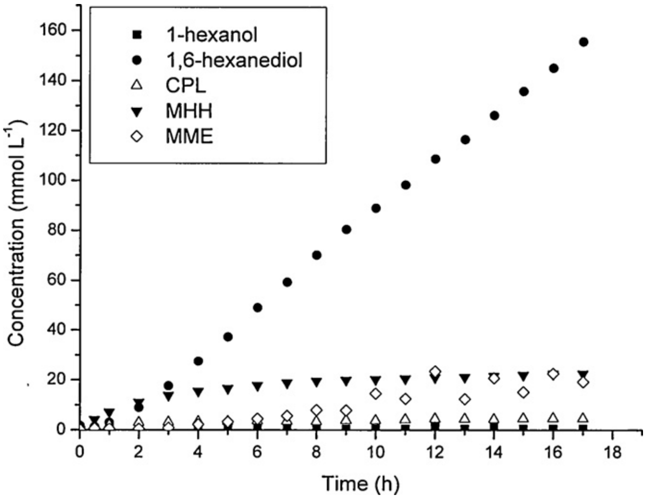

Fig. 13. Products obtained with catalyst RuSn/SiO_2.

The high selectivity to the diol shown by this catalyst could be explained by the stabilization of Sn(II) species on silica in the presence of ruthenium. Another possibility could be a partial reoxidation of metallic tin in the reaction medium, with formation of ionic species in the promoter metal–support interface, before the reaction onset. A similar behavior was observed by Sordelli et al. [38] and Margitfalvi et al. [39] revealing an induction period where the catalyst surface reorganizes and oxidized species of tin would be produced.

The 1-hexanol is probably produced through hydrogenation of diol. It is believed that any decrease in the concentration of diol is observed since this is much higher than 1-ol. There were not observed products such as hexanoic acid or *n*-hexane as well as a decrease of side reactions that lead to the formation of CPL, MHH and MME.

Some of the products formed in the DMA hydrogenation were evaluated as substrates, by using RuSn/SiO_2 as catalyst. When diol was the substrate, the conversion reached 30%, with selectivity of 17.4% for 1-ol and 3.9% for CPL. The results confirm the formation route of 1-ol previously proposed, and suggest the possibility of the formation of CPL also from diol. Thus, in the case of RuSn/La_2O_3 as catalyst, the concomitant formation of diol and CPL may suggest that one or both of them are acting as an intermediate in the reaction. With MME as substrate, the system showed 99% of conversion. After 5 h reaction time over 90% of MME had already been converted to products. The main products were diol, MHH and CPL. The latter two were formed early in the reaction and it was observed a slight reduction in their concentrations, possibly giving rise to diol. These results confirm that MME can act as an intermediate product. When CPL was used as substrate the conversion was practically total, 99%, with 97% of the substrate being consumed after only 2 h reaction time. However, the formation of diol reaches the equilibrium only after 10 h reaction time. A mechanism of diols formation from lactones was proposed by Hamminga et al. [40] and it involves the carbonyl hydrogenation in a first step, making the ring to open to form the diol, with the possibility of formation of hexanoic acid.

The catalysts supported on Nb_2O_5 showed high selectivity to diol. RuSn/Nb_2O_5 catalyst presents a DMA conversion higher than that observed with the Ru/Nb_2O_5 catalyst. It is observed that for both monometallic ruthenium catalysts, Ru/TiO_2–R and Ru/Nb_2O_5, the activities are higher than that observed with Ru/SiO_2 catalyst. This indicates that reducible oxides may contribute to the increased rate of hydrogenation in the absence of a promoter such as tin. Assuming that the oxide Nb_2O_5 is considered reducible oxide [41], the behavior of the bimetallic catalyst is attributed to a possible effect of decoration of metallic sites (Ru(0)) by NbO_x species formed during the reduction of the catalyst. It is also possible the dilution of metal particles by these species [42]. Note also that there was a decrease in the number of products formed by the use of niobia. This result may be associated with the set of effects caused by the decoration effect, as the blocking of active sites that lead to excessive substrate hydrogenation.

Fig. 14 shows the formation of products catalyzed by RuSn/Nb_2O_5. In this case, presented results are obtained within 18 h reaction time. It appears that after 16 h reaction time the concentration of all products, including diol, remains constant. This result may suggest that at this moment there are no metallic ruthenium sites available.

The production of MME can be associated to the presence of metallic sites on the catalyst surface with little or no interaction with tin species. Thus, tin sites location must be appropriate in order to contribute to the selectivity of the reaction and then, to the formation of diol. The close contact of two metals seems to be decisive for the formation of catalytic active sites [43]. According to Galvagno et al. [44] and Kluson and Cervany [26] the effect of activation of tin ions is directly related to the formation and stabilization of ionic species of tin in the vicinity of the active metal atom. This fact explains the effect of the promoter in the hydrogenation of carbonyl by the transfer of hydrogen from adjacent ruthenium sites. Similarly, Silva et al. [14] reported that catalytic active sites presented in RuSn catalysts involve tin in direct contact with Ru(0). Regarding the selectivity of the catalyst RuSn/Nb_2O_5 to diol (50%), it may be related, as in the catalyst RuSn/SiO_2, to an ease interaction between the metals on the supports as observed in TPR. Even though niobia is a reducible oxide, the interaction metal–promoter is preferred to the typical metal–support interaction, behavior also verified by Schmal et al. [42]. In these cases, the chemical nature of the support is fundamental in order to facilitate the formation of active and selective sites.

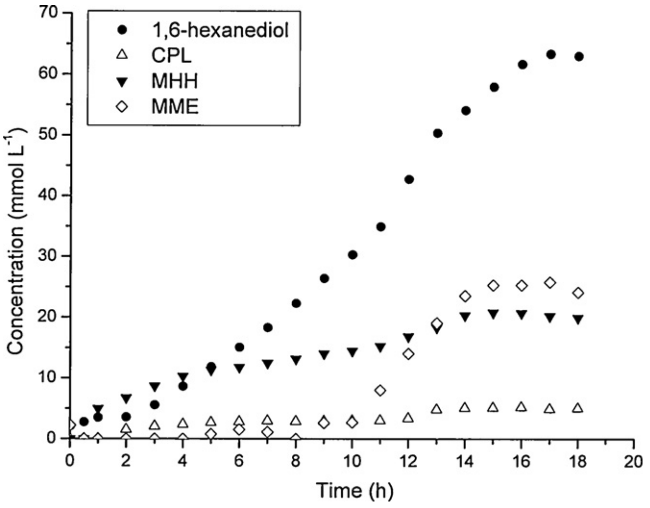

Fig. 14. Products obtained with catalyst RuSn/Nb_2O_5.

4. Conclusions

The catalysts studied in this work presented fundamental differences in behavior for both conversion and selectivity in the formation of 1,6-hexanediol. The presence of tin reduced species is crucial for this selectivity. Without tin the rate of carbonyl hydrogenation was not effective. Reducible oxides used as support are unable to produce sufficient acid strength in order to be selective to diol.

Over RuSn/SiO_2 catalyst, both activity and 1,6-hexanediol selectivity were highest. The use of SiO_2 as support favored the formation of combined active sites between ruthenium and reduced tin species that favored the hydrogenation of the ester group.

Among the reducible metal oxides used as support in this work, all of them subject to the SMSI effect (La_2O_3, TiO_2–R and Nb_2O_5), niobium oxide showed the best results of activity and selectivity to the diol. In the systems supported on Nb_2O_5 it was possible to observe both the enhancing effect of NbO_x species and the decoration effect of metal active sites. The increase in catalytic activity of bimetallic catalysts suggests the creation of sites between ruthenium and tin that interact each other and promote the hydrogenation of dimethyl adipate.

These results indicate that the support on which are dispersed both the active phase and the promoter can change the interaction between them, influencing the formation of active sites and the behavior of the catalyst. It was possible to observe a direct relationship between the reducibility of metal species, the catalytic activity and the selectivity. Thus, a combined effect between support and promoter is essential for obtaining satisfactory results.

Acknowledgements

The authors thank FAPESP (2006/04142-0 and 2009/07109-2), CAPES and CNPq for their financial support, UNICAMP and PUC-Campinas for their support on the development of the studies.

References

[1] M. Toba, S.I. Tanka, S.I. Niwa, F. Mizukami, S. Koppány, L. Guezi, K.Y. Cheah, T.S. Tang, Appl. Catal. 189 (1999) 243–250.
[2] V. Ponec, Appl. Catal. A 149 (1997) 27–48.
[3] S.M. Santos, A.M. Silva, E. Jordão, M.A. Fraga, Catal. Commun. 5 (2004) 377–381.
[4] F.C.A. Figueiredo, E. Jordão, W.A. Carvalho, Catal. Today 223 (2005) 107–108.
[5] A.M. Silva, O.A.A. Santos, M.A. Morales, E.M. Baggio-Saitovitch, E. Jordão, M.A. Fraga, J. Mol. Catal. A 253 (2006) 62–69.
[6] F.C.A. Figueiredo, E. Jordão, W.A. Carvalho, Appl. Catal. A 351 (2008) 259.
[7] G. Ertl, H. Knozinger, J. Weitkamp (Eds.), Preparation of Solid Catalysts, Wiley/VCH, Weinheim, Germany, 1999, p. 442.
[8] S.J. Tauster, S.C. Fung, R.L. Garten, J. Am. Chem. Soc. 100 (1978) 170–175.
[9] T. Uchijima, Catal. Today 28 (1996) 105–117.
[10] I. Nowak, M. Ziolek, Chem. Rev. 99 (1999) 3603–3624.
[11] M.P. Rosynek, D.T. Magnuson, J. Catal. 46 (1977) 402–413.
[12] R.P. Taylor, G.L. Schrader, Ind. Eng. Chem. Res. 30 (1991) 1016–1023.
[13] K. Kontapakdee, J. Panpranot, P. Praserthdam, Catal. Commun. 8 (2007) 2166–2170.
[14] A.M. Silva, O.A.A. Santos, M.J. Mendes, E. Jordão, M.A. Fraga, Appl. Catal. A 241 (2003) 155–165.
[15] M.J. Mendes, O.A.A. Santos, E. Jordão, A.M. Silva, Appl. Catal. A 217 (2001) 253–262.
[16] I.E Wachs, L.E. Briand, J.M. Jehng, L.E. Burcham, X. Gao, Catal. Today 57 (2000) 323–330.
[17] M. Ziolek, Catal. Today 78 (2003) 47–64.
[18] F.B. Noronha, M. Schmal, M. Primet, R. Frety, Appl. Catal. 78 (1991) 125–139.
[19] N. Matsui, K. Anzai, N. Akamatsu, K. Nakagawa, N. Ikenaga, T. Suzuki, Appl. Catal. 179 (1999) 247–256.
[20] B. Klingenberg, M.A. Vannice, Appl. Catal. B 21 (1999) 19–33.
[21] S. Bernal, R. Garcia, J.M. Rodriguez-Izquierdo, J.M. Trillo, J. Less-Common Met. 94 (1983) 145–150.
[22] J.N. Coupé, E. Jordão, M.A. Fraga, M.J. Mendes, Appl. Catal. A 199 (2000) 45–51.
[23] Y. Pouilloux, F. Autin, J. Barrault, Catal. Today 63 (2000) 87–100.
[24] B.A. Riguetto, C.E.C. Rodrigues, M.A. Morales, E. Baggio-Saitovitch, L. Gengembre, E. Payen, C.M.P. Marques, J.M.C. Bueno, Appl. Catal. A: Gen. 318 (2007) 70–78.
[25] J. Llorca, N. Homs, J. León, J. Sales, J.L.G. Fierro, P. Ramirez de la Piscina, Appl. Catal. A 189 (1999) 77–86.
[26] P.E. Kluson, L. Cervany, Appl. Catal. A 128 (1995) 13–31.
[27] K. Tahara, E. Nagahara, S. Itoi, S. Nishiyama, S. Tsuruya, M. Masai, Appl. Catal. A 154 (1997) 75–86.
[28] P. Gallezot, D. Richard, Rev. Sci. Eng. 40 (1998) 81–126.
[29] Y. Pouilloux, F. Autin, C. Guimon, J. Barrault, J. Catal. 176 (1998) 215–224.
[30] S. Mahmoud, A. Hammoudeh, S. Gharaibeh, J. Melsheimer, J. Mol. Catal. A 178 (2002) 161–167.
[31] P. Reyes, M.C. Aguire, J.L.G. Fierro, G. Santori, O. Ferretti, J. Mol. Catal. A 184 (2002) 431–441.
[32] Y. Li, Y. Fan, H. Yang, B. Xu, L. Feng, M. Yang, Y. Chen, Chem. Phys. Lett. 372 (2003) 160–165.
[33] M.A. Vannice, R.L. Garten, J. Catal. 63 (1980) 255.
[34] A. Auroux, D. Sprinceana, A. Gervasini, J. Catal. 195 (2000) 140–150.
[35] F.C.A. Figueiredo, E. Jordão, R. Landers, W.A. Carvalho, Appl. Catal. A 371 (2009) 131–141.
[36] D. Poondi, M.A. Vannice, J. Mol. Catal. A 124 (1997) 79–89.
[37] U. Diebold, Surf. Sci. Rep. 48 (2003) 53–229.
[38] L. Sordelli, R. Psaro, G. Vlaic, A. Cepparo, S. Recchia, C. Dossi, A. Fusi, R. Zanoni, J. Catal. 182 (1999) 186–198.
[39] J.L. Margitfalvi, G.Y. Vankó, I. Borbáth, A. Tompos, A. Vertes, J. Catal. 190 (2000) 474–477.
[40] G.M. Hamminga, G. Mul, J.A. Moulijn, Chem. Eng. Sci. 59 (2004) 5479–5485.
[41] F.B. Noronha, A. Frydman, D.A.G. Aranda, C. Perez, R.R. Soares, B. Morawek, D. Castner, C.T. Campbell, R. Frety, M. Schmal, Catal. Today 28 (1996) 147–157.
[42] M. Schmal, D.A.G. Aranda, R.R. Soares, F.B. Noronha, A. Frydman, Catal. Today 57 (2000) 169–176.
[43] G. Néri, R. Pietropaolo, S. Galvagno, C. Milone, J. Schamank, J. Chem. Soc. 90 (1994) 2803–2807.
[44] S. Galvagno, A. Donato, G. Néri, R. Pietropaolo, G. Capannelli, J. Mol. Catal. 78 (1993) 227–236.